Computer Science and Information Technologies
Vol. 4, No. 3, November 2023, pp. 249~257
ISSN: 2722-3221, DOI: 10.11591/csit.v4i3.p249-257

Hybrid transformation with 1'st order statistics for medical image analysis and classification

Loay E. George[1,2], Maryam Yaseen Abdullah[3], Raghad K. Abdulhassan[3], Asmaa Abdulrazzaq Al_Qaisi[3]
[1]College of Science, University of Baghdad, Baghdad, Iraq
[2]University of Information and Communication Technology, Baghdad, Iraq
[3]Department of Computer Science, College of Education for Women, University of Baghdad, Baghdad, Iraq

Article Info

Article history:

Received Feb 21, 2022
Revised Aug 13, 2023
Accepted Aug 29, 2023

Keywords:

Color image
Discrete cosine transforms
Feature extraction
Gradient
Skin cancer classification
Statistical methods

ABSTRACT

Skin cancer, one of the most critical forms of cancer, required early detection and documentation for efficient treatment, especially as certain types are fatal. In this study, an artificial neural network (ANN) was utilized to discover and index diverse melanomas using the ISIC 2018 dataset. The pre-processing phase is stringent as it insulates the cancerous fraction of a skin image, involving removing, trimming, thinning, and normalizing. In this phase, unwanted hair pieces on the image are eliminated in this phase. Feature extraction from the clipped image is achieved using a discrete cosine transform (DCT) and a gradient transform to transform it into frequency-domain coefficients. Statistical feature extraction is used to reduce the amount of data required for ANN training. A dataset from ISIC 2018 that consists of seven different images from dermoscopic procedures for classification purposes is used in the empirical investigation. An accuracy of 85.44% for DCT in the sub-bands and 76.07% for the sub-band gradient transform was achieved by the applied ANN. The hybrid system's mean squared error (MSE) was discovered to be 3.52×10-4. The work highlights the potential of ANN in the early detection of skin cancer, supporting more efficient treatment and preventing advanced cases.

Corresponding Author:

Asmaa Abdulrazzaq Al_Qaisi
Department of Computer Science, College of Education for Women, University of Baghdad
Baghdad, Iraq
Email: asma_72@coeduw.uobaghdad.edu.iq

1. INTRODUCTION

The most common disease in the world is known for its rising incidence rates and growing effects. Visually distinguishing between benign cancers and aberrant and general cancers might be difficult. Typically, doctors general practitioners (GPs) lack the necessary training to diagnose skin tumors [1]. Because of this, efforts are concentrated on developing and executing cancer detection systems that use a three-step process to detect the borders of lesions using 1'st order statistical characteristics, followed by feature extraction, selection, and classification. Unrestricted, uneven skin cells are what are referred to as skin tumors. When deoxyribonucleic acid or DNA in skin cells is damaged, the modifications or abnormalities that follow allow the skin cells to expand quickly and develop into deadly tumors. Skin malignancies are commonly diagnosed through physical examination and surgery [2]. This operation is a simple outpatient procedure in which the entire or a portion of the afflicted region is removed and tested at a testing facility. medical vision depending on the experiment, dermoscopy is the most successful method for obtaining color skin imaging [3].

The conventional skin cancer databases are modest and only include a few particular subtypes of the illness [4]. New approaches to classifying skin tumors are the goal of research on the most efficient methods of cancer classification. The convolutional neural network (CNN) performs better when working with skin image data that has been produced by flipping and rotating [5]. This is because it allows for inconsistencies between the training and test sets. Neural network (NN) was employed in [6] to classify skin cancer into three groups. Dermoscopy pictures of the kind used in this work quickly operate on skin color photos without any pre-processing. Gessert *et al.* [7] uses the CNN and an extra dense NN to decrease the features. Using external information and the category of skin tumors, this work achieves the goal of explaining the dataset strategy.

Another class lesion concern is the stark disparity in the number of images per class. The input resolutions for the die rent technique and die rent cropping strategies are taken into account in this study to take care of this property, additionally combining information based on age, structural site, sex, and other variables. Using photos of two levels (binary 0 and 1), categorized 3D image shapes have been created in [8]. A novel technique called adaptive snake was utilized to extract the segment features, and the artificial neural network (ANN) was then applied to categorize the segments. The ANN model, which makes use of numerous neural layers, is designed to provide accurate representations of data. The following are requirements for using ANNs: i) the decrease of huge data pertaining to cancer for the training and modeling of NN; ii) the creation of a graphics processing units for device analysis; iii) the adjustment of linear unit and dropping out; and iv) routine normalization in ANN approaches [9].

Identifying malignancies using dermoscopy color images presents a number of intriguing difficulties. First off, it might be difficult to identify skin lesions because of their wide range in size, texture, color, and shape. Second, the categorization process is made more difficult by the significant correlation between melanoma and non-melanoma lesions. Last but not least, environmental variables, including hair, veins, noise, and light, can influence how accurately a tumor is identified [10]–[12]. This study used a variety of feature extraction approaches as a component of the initial processing step to solve these problems. There were two cascade feature extraction techniques. To extract pertinent characteristics from the images. The transformer technique, discrete cosine transform (DCT), discrete wavelet transform (DWT), and gradient approach were employed in the first strategy.

In order to simplify the data and identify key aspects, the second method concentrated on statistical computations such as mean, standard deviation, skewness, and fourth momentum. The obtained data was then used to train an ANN to recognize and classify various types of skin cancer. The goal of this strategy was to use the classification process to arrive at an accurate diagnosis.

2. MATHEMATICAL METHODS FOR IMAGE PROCESSING

There are some mathematical approaches employed for processing images. The DCT, which transform signals from the domain of spatial distribution to a frequency domain; the image gradient, which measures the change in color or intensity in an image; and the 1'st order statistical statistics, which establishes a number of descriptive metrics of the image data. Additionally, for ANNs, which are a class of artificial intelligence models motivated by the design and operation of the human brain, all methods will explain the following.

2.1. Discrete cosine transform

A signal from the spatial to the frequency domain is converted using the DCT in algebra [13], [14]. It is derived from the discrete Fourier transform's (DFT) real portion. According to the DCT, the rebuilt image is displayed with high-frequency components in the bottom right corner and low-frequency components in the top left [15]. Each pixel in the image with the size $N \times M$ is represented by its $p(x, y)$ coordinates. To get the $P\ (u, v)$ DCT coefficients, the two-dimensional DCT is applied to the image.

$$P\ (u,v) = \frac{1}{\sqrt{M+N}} C(u)C(v)\ \sum_{x=0}^{N}\sum_{y=0}^{M} p(i,j) Cos\left(\frac{(2x+1)2\pi}{2N}\right) Cos\left(\frac{(2y+1)2\pi}{2M}\right) \quad (1)$$

$$C(u), C(v) = \begin{bmatrix} 1/\sqrt{2} & u, v = 0 \\ 1 & u, v \neq 0 \end{bmatrix} \quad (2)$$

2.2. Image gradient

The process of changing the color pixel values is referred to as "color gradation" in the context of image processing. Each point in the image, represented by the letters $p(x, y)$, can have its gradient of a dimensional function calculated. The outcome of the gradient computation is a two-dimensional vector that is

composed of the vertical component $g_v(i,j)$ and the horizontal component $g_v(x,y)$, which represent the derivatives in the vertical and horizontal directions at the specified coordinates (x,y) inside the picture [16]. Each pixel's value and how they are dispersed within a sub-block with the dimensions (3*3) determine the values of the gradient vector [17], [18]. The gradient is determined by splitting the image's pixels, $p(x,y)$, into two vectors. $A(x,y)$ and $M(x,y)$, respectively [16].

$$g_v(x,y) = p(x-1,y+1) + 2p(x,y+1) + p(x+1,y+1) - p(x-1,y-1) - 2p(x+1,y-1) - p(x+1,y-1) \quad (3)$$

$$g_h(x,y) = p(x-1,y-1) + 2p(x-1,y+1) + p(x-1,y+1) - p(x+1,y-1) - 2p(x+1,y) - p(x+1,y+1) \quad (4)$$

$$M(x,y) = \sqrt{gv(x,y)^2 + gh(x,y)^2} \quad (5)$$

$$A(x,y) = tan^{-1}\left(\frac{g_v(x,y)}{g_h(x,y)}\right) \quad (6)$$

2.3. The 1'st-order statistical statistics

In order to extract pertinent features from the data, many statistical techniques have been used in the study of skin tumor images [17]. Measuring the color means, variances, skewness, and fourth moments are some of these techniques. The references [18]–[20] from which the statistical equations used in this investigation were derived The chosen equations can effectively characterize image information since they are simple and have the property of being invariant to transform coefficients.

– Mean: the mean for image have size $(N \times M)$ is (7):

$$Mean = \frac{1}{N \times M}\sum_{x=1}^{N}\sum_{y=1}^{M} p(x,y) \quad (7)$$

– Standard deviation is (8):

$$Std = \sqrt{\frac{1}{N \times M}\sum_{x=1}^{N}\sum_{y=1}^{M}(p(x,y) - mean)^2} \quad (8)$$

– Skewness is (9):

$$Skewness = \frac{1}{N \times M}\sum_{x=1}^{N}\sum_{y=1}^{M}(p(x,y) - Mean)^3 \quad (9)$$

– Fourth momentum (kurtosis) is (10)

$$Fourth\ Moment = \frac{1}{N \times M}\sum_{x=1}^{N}\sum_{y=1}^{M}(p(x,y) - Mean)^4 \quad (10)$$

Contrast [21]: the segmented sub-region of size $(n * n)$ by (11):

$$Contrast = \sum_{x=1}^{n}\sum_{y=1}^{n}\frac{|p(x,y) - mean_{n*n}|}{Std_{n*n}} \quad (11)$$

Michelson contrast is (12):

$$\frac{I_{max} - I_{min}}{I_{max} + I_{min}} \quad (12)$$

2.4. Artificial neural networks

The input layer, the output layer, and a number of hidden layers make up the three ANN [21]. The network's accuracy is determined by the training procedures, which depend on the importance of the features, including the statistical or gradient techniques (applied in this work) [22]. The network is built using computed layer weight values to lessen the difference between calculated results and predicted values. Repeated calculations are used to update these values. This problem is referred to as the vanishing gradient [23]–[25].

3. PROPOSED METHOD

This study introduced a novel method that combines DCT with gradient descent approaches. Then, for comparative analysis, this hybrid method is used with a variety of state-of-the-art skin image categorization methods. The three main steps that make up the proposed system are feature extraction, classification, and image preprocessing. The block diagram of the suggested system, shown in Figure 1, illustrates these phases. The system works in a cascading process, with each phase following the previous one. A perfect transition and efficient processing of one phase to the next are ensured by this consecutive action. The efficiency of this cascading technique is proved by the findings of the comparison analysis, which show how all three phases are interconnected and how each contributes to the overall performance of the entire system.

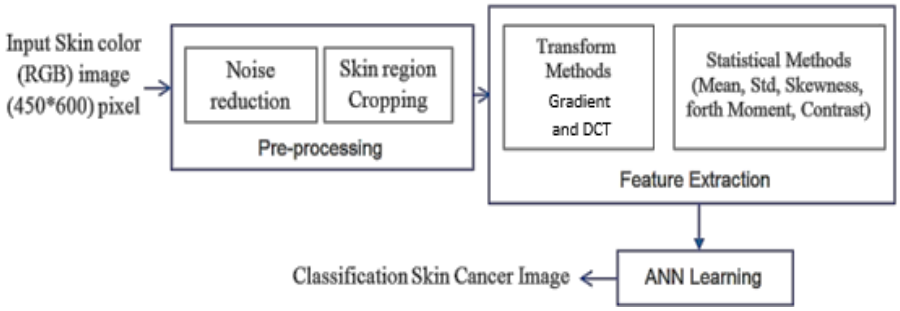

Figure 1. Skin cancer methods for classification in a block diagram

3.1. Image preprocessing for color image

The preprocessing steps to isolate the malignant component from other skin areas are: i) noise removal: in this case, unwanted pixels from the red, green, and blue (RGB) photos, such as hair, are eliminated using median filter; ii) cropping: we are interested in the cancer industry. The white areas surrounding cancer have been reduced; iii) thinning: by eliminating a few foreground pixels, cancer strokes are made to have the smallest possible cross–sectional width; and iv) normalization: from all three 128×128-pixel RGB images. Only the cancer patches are clipped. The entire preparation process is depicted in Figure 2.

Figure 2 illustrates the process of cancer image analysis and modification where Figure 2(a) shows the original cancer imager. Figures 2(b)-(d) show the application of median filtering on the image, thinning of the cancer area, and outlining of the cancer region. Figures 2(e) dan 2(f) show the normalization of the cropped image and reduction of the cancer region to a 128×128 resolution.

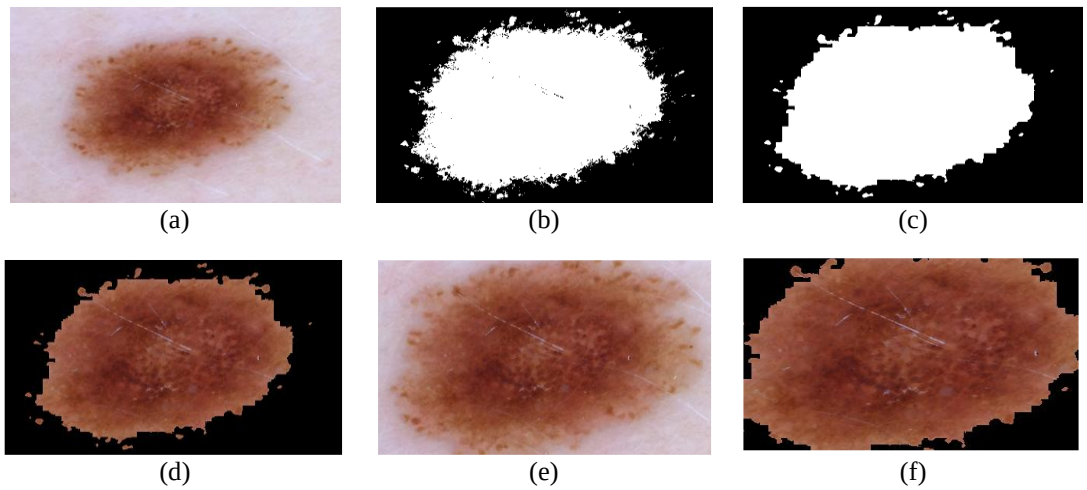

Figure 2. The overall preprocessing procedure (a) a cancer image, (b) the median filtering on the picture, (c) thinner of the cancer area, (d) outlining of the cancer region, (e) normalization of the cropped image, and (f) reduction of the cancer region to 128×128

3.2. Feature extraction

3.2.1. The initial phase

Two different transformations, the DCT and the gradient, have been performed on the normalization trim cancer area in order to identify, retrieve, and adjust pixel differences in the RGB image. The proposed method uses a DCT approach for each sub-band in RGB images to break the cropped photos into sub-bands (8*8), allowing for the extraction of features from the surrounding environment. Figure 3 demonstrates the application of the DCT on cropped images divided into 8×8 pixel sub-bands and the stages of this process for a normalized cancer image where Figure 3(a) shows an original image. Figures 3(b)-(d) show the red image coefficient, green image coefficient, and blue image coefficient.

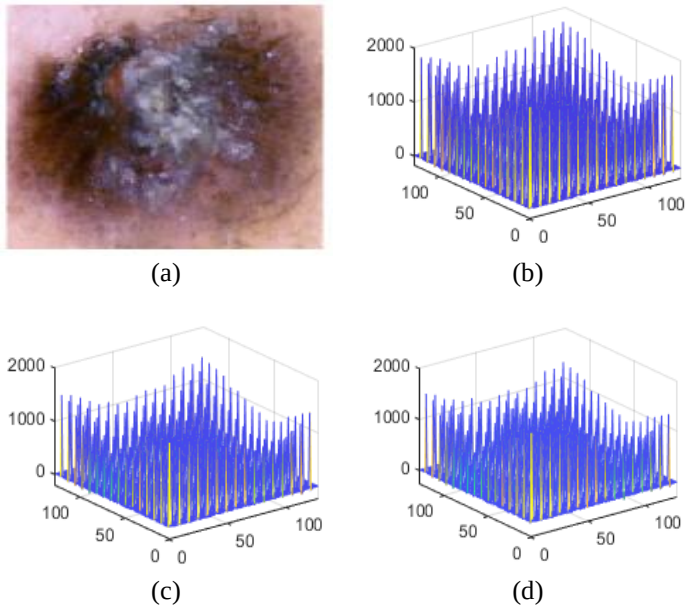

Figure 3. Image of the sub-block DCT for normalized cancer (a) original image, (b) the red image coefficient, (c) the green image coefficient, and (d) the blue image coefficient

In order to show a wide range of colors, RGB graphics use three color channels: red, green, and blue. The total number of frequency components extracted from the image after a particular transform is performed is referred to as the 8*8 sub-band. As demonstrated in Figure 4, in order to show a wide range of colors, RGB graphics use three color channels: red, green, and blue. The total number of frequency components extracted from the image after a particular transform is performed is referred to as the "8*8" sub-band (Figure 4). This figure shows the gradient transform's magnitude for three distinct images created using a normalized cancer image. Each of these images represents a different aspect of the cancer image. Where Figure 4(a) shows the red image. Figures 4(b) and (c) shows the green image and the blue image.

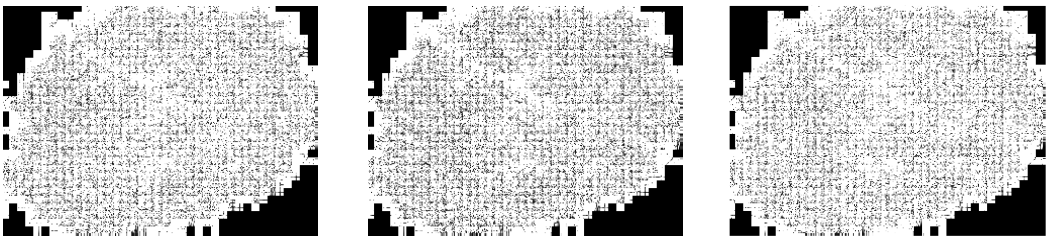

Figure 4. The gradient transform's magnitude for three distinct images created using a normalized cancer image (a) the red image, (b) the green image, and (c) the blue image

3.2.2. The second phase

Mean, standard deviation, skewness, and fourth momentum were used to determine the contrast of the cancer selected picture was computed for the RGB coefficient discoveries in DCT and gradient. The hybrid block diagram and feature vector, respectively, are shown in Figures 5 and 6. This phase helps with data collection and reduces the amount of information needed for learning.

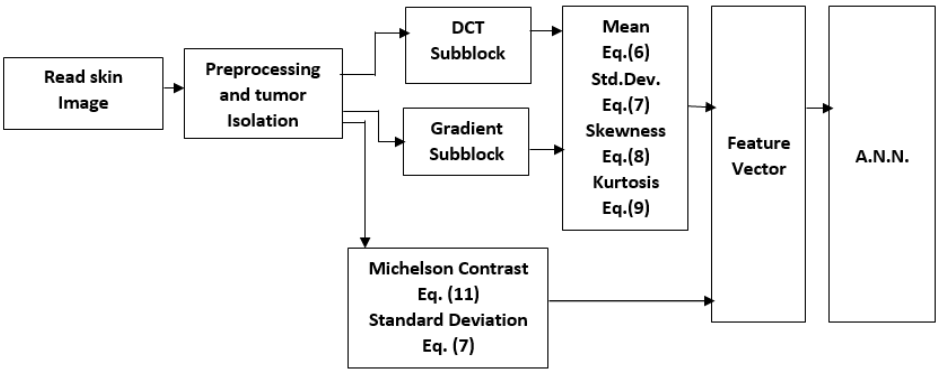

Figure 5. The hybrid block diagram

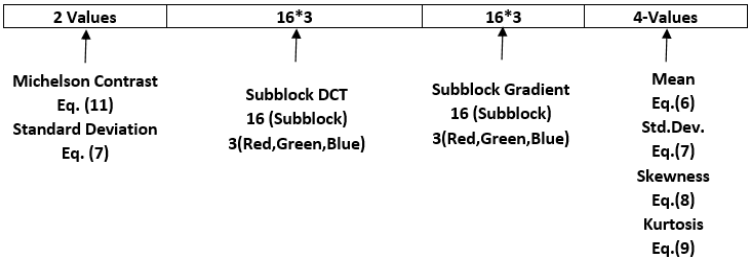

Figure 6. The feature vector

3.3. Artificial neural network

A backpropagation method has been developed for the detection of skin malignancies. Each of the two hidden layers in the ANN contains 20 nodes. The 200 iterations have reduced the error.

4. RESULT OF THE PROPOSED SYSTEMS

The suggested approach has been used to create several categorization ANN networks. Both the sub-band gradient transform and the sub-band DCT use the suggested feature extraction method. The minimum number of features was extracted in the second stage using a five-statistic computation (each color image has 3×5=15 feature values). The 30% of the data was used for testing, while 70% was used for training. The mean square error (MSE) for the ANN train is displayed in Table 1.

Table 2, which shows how the images of skin cancer are arranged in a complicated matrix, seems inconsistent. In Table 3, the two distinct skin cancer classification algorithms that were created with the use of this matrix are described. Figure 7 shows how the ANN performed when learning the DCT and gradient during the training phase. The capacity of the ANN to classify skin cancer using features taken using DCT and gradient is clearly seen in this figure. These figures and tables provide a thorough explanation of the creation and operation of the skin cancer categorization algorithms. The discrepancies found in Table 2 point to possible directions for future research that could be improved.

Table 1. The MSE of the offered methods' ANN train is employed

No.	Proposed method	MSE
1	Methods for sub-band gradients	$12*10^{-4}$
2	Sub-band DCT methods	$7*10^{-4}$

Table 2. Results of DCT with gradient with contrast and 1'st order statistics

Tumor types	Total image	Detection ratio
1	327	82%
2	514	86%
3	1099	76%
4	115	89%
5	6705	93%
6	1113	70%
7	140	93%

Table 3. The confusing matrix for DCT+ gradient+ contrast (Hybrid) method

Parameter	Tumor types	Predicted tumor types						
		1	2	3	4	5	6	7
Actual tumor types	1	268	48	9	2	0	0	0
	2	18	441	48	7	0	0	0
	3	0	63	839	191	6	0	0
	4	0	1	9	102	3	0	0
	5	0	0	45	235	6220	215	0
	6	0	0	10	110	162	774	57
	7	0	0	0	1	1	8	130

		Predicted tumor types	
		Positive	Negative
Actual tumor types	Positive	6695	328
	Negative	913	2079

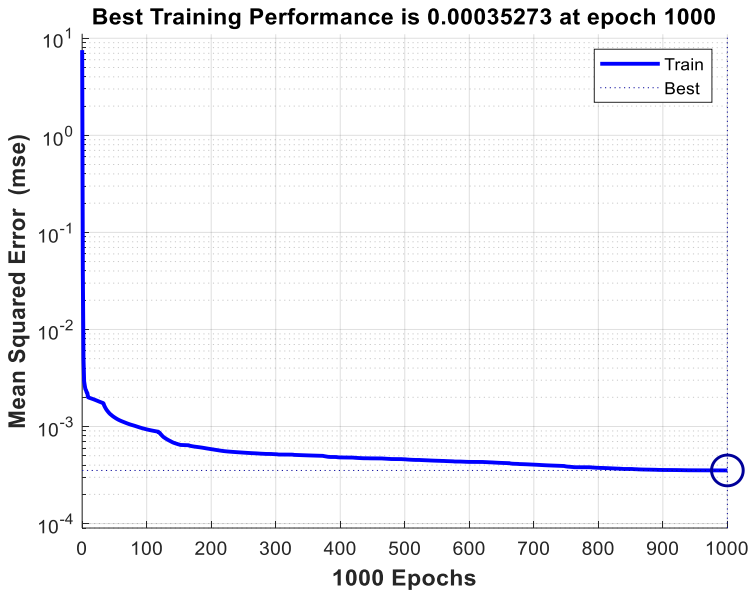

Figure 7. The ANN train performance for DCT+ gradient (Hybrid) feature extraction for 1000 epoch, the MSE =3.52×10^{-4}

5. CONCLUSION

There has been a great deal of research into the use of medical imaging to identify melanoma, a type of skin cancer. The use of the DCT sub-band was one of the ways that was tried, but regrettably, it had lower accuracy rates and higher error detection than methods that combine feature extraction with ANN. The disparity in the dataset used to train the models is a key obstacle in this sector. The dataset includes images that have been divided into various classes according to the characteristics of the lesion, although there is an obvious difference in the number of images that are accessible for each class. This difference makes it difficult to classify lesion image attributes accurately. However, it was shown that combining gradient and DCT approaches produced a more successful method. The effectiveness of training the ANN was greatly increased by this combination. The MSE, a metric of the model's performance, was specifically lowered toa value of 3.5210-4 after 1000 epochs. This shows that this combination strategy for cancer image categorization delivers great accuracy and efficiency.

REFERENCES

[1] M. A. A. Milton, "Automated skin lesion classification using ensemble of deep neural networks in ISIC 2018: skin lesion analysis towards melanoma detection challenge," *arXiv.org*, Jan. 2019.

[2] T. Y. Satheesha, D. Satyanarayana, M. N. Giriprasad, and K. N. Nagesh, "Detection of melanoma using distinct features," in *2016 3rd MEC International Conference on Big Data and Smart City (ICBDSC)*, IEEE Xplore, Mar. 2016, pp. 1–6, doi: 10.1109/ICBDSC.2016.7460367.

[3] K. M. Hosny, M. A. Kassem, and M. M. Foaud, "Skin melanoma classification using deep convolutional neural networks," in *Deep Learning in Computer Vision*, 1st Edition., CRC Press, 2020, pp. 1–24.

[4] S. S. Han, M. S. Kim, W. Lim, G. H. Park, I. Park, and S. E. Chang, "Classification of the clinical images for benign and malignant cutaneous tumors using a deep learning algorithm," *Journal of Investigative Dermatology*, vol. 138, no. 7, pp. 1529–1538, Jul. 2018, doi: 10.1016/j.jid.2018.01.028.

[5] N. C. F. Codella *et al.*, "Skin lesion analysis toward melanoma detection: a challenge at the 2017 international symposium on biomedical imaging (ISBI), hosted by the international skin imaging collaboration (ISIC)," *arXiv.org*, Oct. 2017.

[6] R. S. S. Sundar and M. Vadivel, "Performance analysis of melanoma early detection using skin lession classification system," in *2016 International Conference on Circuit, Power and Computing Technologies (ICCPCT)*, Mar. 2016, pp. 1–5, doi: 10.1109/ICCPCT.2016.7530182.

[7] N. Gessert, M. Nielsen, M. Shaikh, R. Werner, and A. Schlaefer, "Skin lesion classification using ensembles of multi-resolution EfficientNets with meta data," *MethodsX*, vol. 7, 2020, doi: 10.1016/j.mex.2020.100864.

[8] S. M. Kumar, J. R. Kumar, and K. Gopalakrishnan, "skin cancer diagnostic using machine learning techniques – shearlet transform and naïve bayes classifier," *International Journal of Engineering and Advanced Technology (IJEAT)*, vol. 9, no. 2, pp. 3478–3480, 2019.

[9] N. S. Athi, "Program for color image segmentation." in *MathWorks*. K.S.R College of Engineering, Erode, Tamil Nadu, India, Jun. 2011.

[10] H. A. Haenssle *et al.*, "Man against machine: diagnostic performance of a deep learning convolutional neural network for dermoscopic melanoma recognition in comparison to 58 dermatologists," *Annals of Oncology*, vol. 29, no. 8, pp. 1836–1842, Aug. 2018, doi: 10.1093/annonc/mdy166.

[11] C. Barata, M. E. Celebi, and J. S. Marques, "A survey of feature extraction in dermoscopy image analysis of skin cancer," *IEEE Journal of Biomedical and Health Informatics*, vol. 23, no. 3, pp. 1096–1109, May 2019, doi: 10.1109/JBHI.2018.2845939.

[12] M. K. Monika, N. A. Vignesh, Ch. U. Kumari, M. N. V. S. S. Kumar, and E. L. Lydia, "Skin cancer detection and classification using machine learning," *Materials Today: Proceedings*, vol. 33, pp. 4266–4270, Jan. 2020, doi: 10.1016/j.matpr.2020.07.366.

[13] A. Seal, D. Bhattacharjee, and M. Nasipuri, "Predictive and probabilistic model for cancer detection using computer tomography images," *Multimedia Tools and Applications*, vol. 77, no. 3, pp. 3991–4010, Feb. 2018, doi: 10.1007/s11042-017-4405-7.

[14] T. J. Brinker *et al.*, "Skin cancer classification using convolutional neural networks: systematic review," *Journal of Medical Internet Research*, vol. 20, no. 10, Oct. 2018, doi: 10.2196/11936.

[15] H. Nahata and S. P. Singh, "Deep learning solutions for skin cancer detection and diagnosis," in *Machine Learning with Health Care Perspective: Machine Learning and Healthcare*, V. Jain and J. M. Chatterjee, Eds., in Learning and Analytics in Intelligent Systems. Cham: Springer International Publishing, 2020, pp. 159–182, doi: 10.1007/978-3-030-40850-3_8.

[16] M. A. M. Almeida and I. A. X. Santos, "Classification models for skin tumor detection using texture analysis in medical images," *Journal of Imaging*, vol. 6, no. 6, Jun. 2020, doi: 10.3390/jimaging6060051.

[17] P. Tschandl, C. Rosendahl, and H. Kittler, "The HAM10000 dataset, a large collection of multi-source dermatoscopic images of common pigmented skin lesions," *Scientific Data*, vol. 5, no. 1, Aug. 2018, doi: 10.1038/sdata.2018.161.

[18] M. Combalia *et al.*, "BCN20000: dermoscopic lesions in the wild," *arXiv.org*, Aug. 2019.

[19] R. M. Haralick, "Statistical and structural approaches to texture," *Proceedings of the IEEE*, vol. 67, no. 5, pp. 786–804, May 1979, doi: 10.1109/PROC.1979.11328.

[20] N. B. Bahadure, A. K. Ray, and H. P. Thethi, "Image analysis for MRI based brain tumor detection and feature extraction using biologically inspired BWT and SVM," *International Journal of Biomedical Imaging*, vol. 2017, 2017, doi: 10.1155/2017/9749108.

[21] M. Abdel-Nasser, A. Moreno, and D. Puig, "Breast cancer detection in thermal infrared images using representation learning and texture analysis methods," *Electronics*, vol. 8, no. 1, Jan. 2019, doi: 10.3390/electronics8010100.

[22] S. Ayyachamy, "Registration based retrieval using texture measures," *Applied Medical Informatics*, vol. 37, no. 3, pp. 1–10, 2015.

[23] ISIC, "International skin imaging collaboration challenge." Accessed: Feb. 12, 2019. [Online]. Available: https://challenge.isic-archive.com/landing/2019/

[24] T. J. Brinker *et al.*, "Deep learning outperformed 136 of 157 dermatologists in a head-to-head dermoscopic melanoma image classification task," *European Journal of Cancer*, vol. 113, pp. 47–54, May 2019, doi: 10.1016/j.ejca.2019.04.001.

[25] A. Hekler *et al.*, "Pathologist-level classification of histopathological melanoma images with deep neural networks," *European Journal of Cancer*, vol. 115, pp. 79–83, Jul. 2019, doi: 10.1016/j.ejca.2019.04.021.

BIOGRAPHIES OF AUTHORS

Dr. Loay E. George is an assistant professor at the University of Information Technology and Communications (UOITC) and the assistant of the University President for scientific affairs. He has a Ph.D. in physics, which he obtained in 1979. He has been a faculty member at the College of Science, University of Baghdad, Iraq, before joining UOITC. His main research interests include: digital multimedia processing, pattern recognition, and classification. He can be contacted at email: loayedwar57@uoitc.edu.iq.

Maryam Yaseen Abdullah received the bachelor's degree in computer science from the College of Education for Women at the University of Baghdad in 2006. She received a master's degree in information technology (IT) from the Faculty of Information Science and Technology (FTSM) at the National University of Malaysia (UKM), Malaysia in 2015. Currently, she is a lecturer in the Department of Computer at the College of Education for Women, University of Baghdad, Iraq. Her research interests include NLP, handwriting recognition, and demonstrating its potential for real-time applications. She can be contacted at email: maryam84@coeduw.uobaghdad.edu.iq.

Raghad K. Abdulhassan works at the University of Baghdad, College of Education for Women, Department of Computer Science. She obtained her bachelor's degree from University of Baghdad-College of Science, Department of Computer Science, in 2000. She also holds a master's degree from University of Baghdad College of Science, Department of Computer Science, in 2014. Her main research interests focus on artificial intelligence, data mining. She can be contacted at email: raghad.k@coeduw.uobaghdad.edu.iq.

Dr. Asmaa Abdulrazzaq Al_Qaisi is an assistant professor in Department of Computer Science at the College of Education for Women, University of Baghdad. She earned her bachelor's degree in Computer Science from Al-Mustansiriya University in 2000, her master's degree in computer science from the University of Technology, Department of Applied Science, in 2014, and her Ph.D. in computer science from the Informatics Institute for Postgraduate Studies in 2022. Her main research areas are bioinspired computing, artificial intelligence, analytical modeling and optimization, information retrieval, and data mining. She can be contacted at email: asma_72@coeduw.uobaghdad.edu.iq.